Special Feature: Spatial Information Technology towards Intelligent Vehicle Systems

Research Report

Precise Dead-reckoning Based on Multi-sensor Fusion

Kojiro Takeyama and Yoshiko Kojima

Report received on Jan. 29, 2018

ABSTRACT In this study, a method of accurate dead reckoning in urban environments via integration of a mono-camera, an IMU (gyro, wheel odometer), and GPS is proposed. Recently, robust and accurate vehicle position information has become essential for driver-assistance systems. In particular, dead reckoning plays an important role for the continuous positioning in areas, such as urban canyons, in which GPS positioning is limited. Visual odometry (VO) using a mono-camera is a method of dead reckoning which offers the potential of low cost and high performance, but has an accumulated heading error along the distance traveled. This study presents a method of heading estimation using GPS Doppler which corrects the accumulated heading error of VO. The key point in this study is the time-series tightly coupled integration of GPS Doppler and IMU that contributes to the improvement of availability of heading correction in an area of poor satellite reception, where heading estimation is not available by GPS Doppler only. As a result of evaluation in an urban environment, the error of dead reckoning is reduced to approximately 1/4, as compared to the conventional method, owing to the improvement and availability of heading correction in the urban environment.

KEYWORDS Visual-odometry, GPS Doppler, Tightly Coupled Integration, Urban Environment, Dead Reckoning, Heading Estimation

1. Introduction

Seamless and accurate positioning of a land vehicle is one of the most important tasks in the development of advanced driver assistance systems. Satellite navigation systems such as GPS are a well-recognized approach for obtaining the position of a vehicle. Real-time kinematic GPS (RTK-GPS)[1] can provide sub-decimeter positioning accuracy in open-sky areas, whereas in urban canyons, the availability of accurate positioning may be greatly reduced owing to the blockage or reflection of satellite signals by tall buildings.

Thus, in areas where accurate absolute positioning is not available, dead reckoning is necessary for seamless positioning. Dead reckoning is a technique that calculates the positional change of a vehicle based on the motion of the vehicle and enables seamless positioning during the intervals between the absolute positions (**Fig. 1**).

There are a variety of approaches to dead reckoning. **Figure 2** shows the feature of major sensors used for dead reckoning. LIDAR[2,3] and fiber-optic gyros are reliable but costly, whereas microelectromechanical systems (MEMS) gyros are much cheaper but have a bias error which changes unpredictably over time.

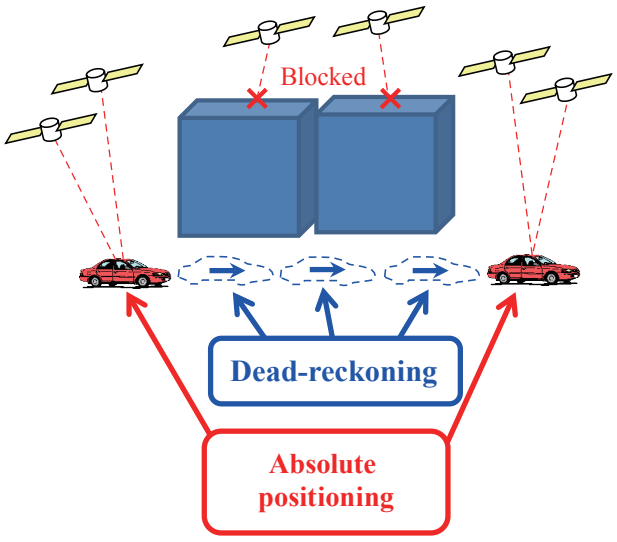

Fig. 1 Absolute positioning and dead reckoning.

On the other hand, visual odometry (VO) using a mono-camera[4,5] has become an attractive approach to dead reckoning due to its potential for high accuracy and reasonable cost. VO is a method that estimates the vehicle trajectory based on the motion of static objects in successive camera images. VO can estimate vehicle trajectory precisely. In addition, sensor costs are decreasing as cameras become standard equipment on modern vehicles. On the other hand, VO has a problem in that the estimation error of the heading is accumulated over time because it cannot estimate the absolute heading, and this results in increased trajectory error. Therefore, the purpose of the present study is to improve the heading of VO using low-cost sensors.

Various studies investigated the issue of heading error. Heng[6] used a magnetometer to correct the accumulated heading error of the VO, but the measurements of a magnetometer occasionally have errors caused by interference with surrounding steel objects, such as street lights or railways. There are also approaches to absolute heading estimation that use GPS signals. Rehder[7] has corrected the heading error of VO through comparison of the time-series vehicle position obtained by GPS and the VO trajectory. Rehder's heading correction approach works well under open-sky conditions, but both the availability and accuracy of heading correction are much degraded in urban environments owing to the blockage or reflection of satellite signals. Meguro[8] used the Doppler shift of the satellite, which can accurately provide the absolute heading of the vehicle, to correct the heading error of VO, but this is also problematic due to limited availability in urban environments. Alonso[9] used a digital road map for heading correction of VO, which works well even in urban environments, although there is a problem with the cost required to generate a sufficiently wide and accurate digital road map.

The present study introduces a robust and accurate heading correction technique achieved by the integration of low-cost sensors (such as mono-cameras, gyros, and wheel odometer GPS) to improve VO in urban environments.

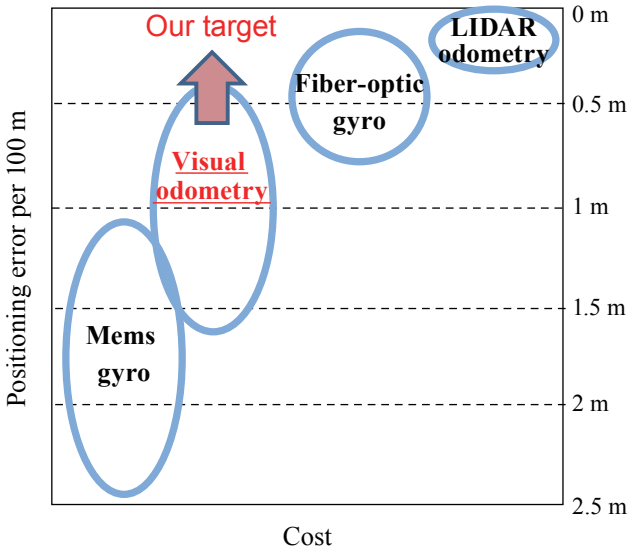

Fig. 2 Feature of major sensors used for dead reckoning.

2. Visual Odometry

Before explaining the proposed method, the basic approach of VO is described in this section. VO estimates vehicle trajectory based on the position change of static objects in sequential images. **Figure 3** presents an overview of VO. First, the feature points of the objects in the images are extracted. The feature points are then tracked along multiple time epochs. The tracked feature points are referred to collectively as the optical flow (OF) and indicate the motion of the objects. Based on the OF, the position and the pose of the vehicle and the 3D position of the feature points are estimated simultaneously.

Equation (1) defines the relationship between vehicle positions, vehicle poses, 3D positions of feature points, and the observed 2D positions of the feature points in the images:

$$\mathbf{X'}_{t,m} = \mathbf{K}\mathbf{R}_t\,[\mathbf{I}|-\mathbf{x}_t]\,\mathbf{X}_m\,, \tag{1}$$

where t is the index of time, m is the index of feature points, $\mathbf{X'}_{t,m}$ is the 2D position of feature points in the images, $\mathbf{K}$ is the matrix of camera calibration parameters, $\mathbf{R}_t$ is the rotation matrix based on the vehicle pose, $\mathbf{I}$ is the identity matrix, $\mathbf{x}_t$ is the vehicle position, and $\mathbf{X}_m$ is the feature point position in 3D space. The operator [A|B] means that matrices A and B are combined. In Eq. (1), $\mathbf{x}_t$, $\mathbf{R}_t$ and $\mathbf{X}_m$ are unknown parameters, and all of the other parameters are observable values. In the present study, bundle adjustment[10] was used to solve the optimization problem of the time-series observation equations. Equation (2) defines the least squares cost function used to solve Eq. (1):

$$E_{cam}(\mathbf{R}_t, \mathbf{x}_t, \mathbf{X}_m) = \sum_{t=0}^{N} \sum_{m=0}^{M} (\mathbf{X'}_{t,m} - \mathbf{K}\mathbf{R}_t [\mathbf{I}| - \mathbf{x}_t] \mathbf{X}_m)^2 , \quad (2)$$

where N is the total number of epochs of the time-series data, and M is the total number of feature points appearing in the time-series data. Here, the Levenberg-Marquardt algorithm[11] is used to solve Eq. (2). This is a widely used algorithm that generates a least-squares solution to nonlinear equations using a convergence operation. In this process, the solutions that minimize E_{cam} are estimated, and, as a result, the vehicle trajectory $\mathbf{x}_t$ is obtained.

3. Proposed Method

3. 1 Overview

VO can estimate highly precise trajectories over short distances, whereas over long distances the heading estimation error can become large, which induces a large trajectory error.

The present study introduces a VO method for heading correction using the Doppler shift of a satellite signal (GPS Doppler) which can robustly work in urban environments. **Figure 4** shows an overview of the proposed method. The key technique is heading correction using the absolute heading estimated by time-series tightly coupled integration of GPS Doppler and IMU (gyro, wheel odometer). While the conventional method requires at least four satellites for heading estimation, the proposed method enables heading estimation with fewer than four satellites. In the present study, the velocity of the vehicle estimated using GPS Doppler is also used for sensor calibration of IMU. In this section, the conventional method of velocity estimation using GPS Doppler is first presented (Sec. 3. 2), and the method of IMU sensor calibration is then described (Secs. 3. 3, 3. 4). The method of absolute heading estimation using the proposed method (Sec. 3. 5) and the method of VO heading correction (Sec. 3. 6) are then shown.

3. 2 Conventional Method of Velocity Estimation Using GPS Doppler

GPS Doppler can estimate vehicle speed very accurately. This section describes the conventional solution for velocity estimation using GPS Doppler.[12,13] **Figure 5** shows an image of GPS Doppler velocity estimation. First, based on GPS Doppler, the relative velocity between each satellite and the vehicle can be calculated, and by subtracting the velocity of the satellite from the relative velocity between the satellite and the vehicle, the vehicle speed in the direction of the satellite is obtained. Then, by combining vehicle speed in the direction of a satellite over multiple satellites, a 3D velocity vector of the vehicle can be calculated.

The following equation describes the relationship between GPS Doppler and the 3D velocity of the vehicle:

$$\frac{D_i}{f1} c + \mathbf{G}_i \cdot \mathbf{vs}_i = \mathbf{G}_i \cdot \mathbf{v} - c\rho$$

$$\mathbf{G}_i = \frac{1}{r_i} (\mathbf{xs}_i - \mathbf{x}) \qquad (i = 1, ..., N) , \quad (3)$$

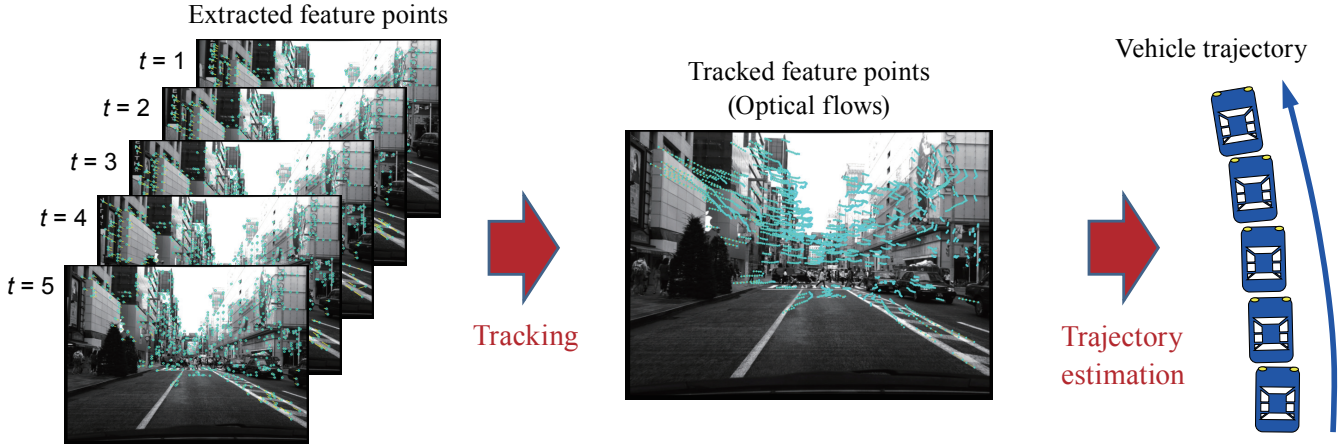

Fig. 3 Process of VO.

where i is the index of the satellites, N is the number of observable satellites in the current epoch, D_i is the GPS Doppler signal of a satellite, c is the speed of light, $f1$ is the frequency of the carrier signal, $\mathbf{G}_i$ is the unit vector of the direction from the vehicle to the satellite (no unit of quantity required), $\mathbf{vs}_i$ and $\mathbf{v}$ are the 3D velocity vectors of a satellite and the vehicle, respectively, and ρ is the clock drift, which is the rate of the receiver clock error variation per second (no unit of quantity required). Here, $\mathbf{G}_i$ can be calculated based on the satellite position $\mathbf{xs}_i$, the vehicle position $\mathbf{x}$, and the distance between the vehicle and the satellite r_i.

In Eq. (3), the unknown parameters are $\mathbf{V}$ (3D vector of vehicle velocity) and ρ (clock drift), and all others are observable values. Thus, the number of unknowns is four, and the number of equations is dependent on

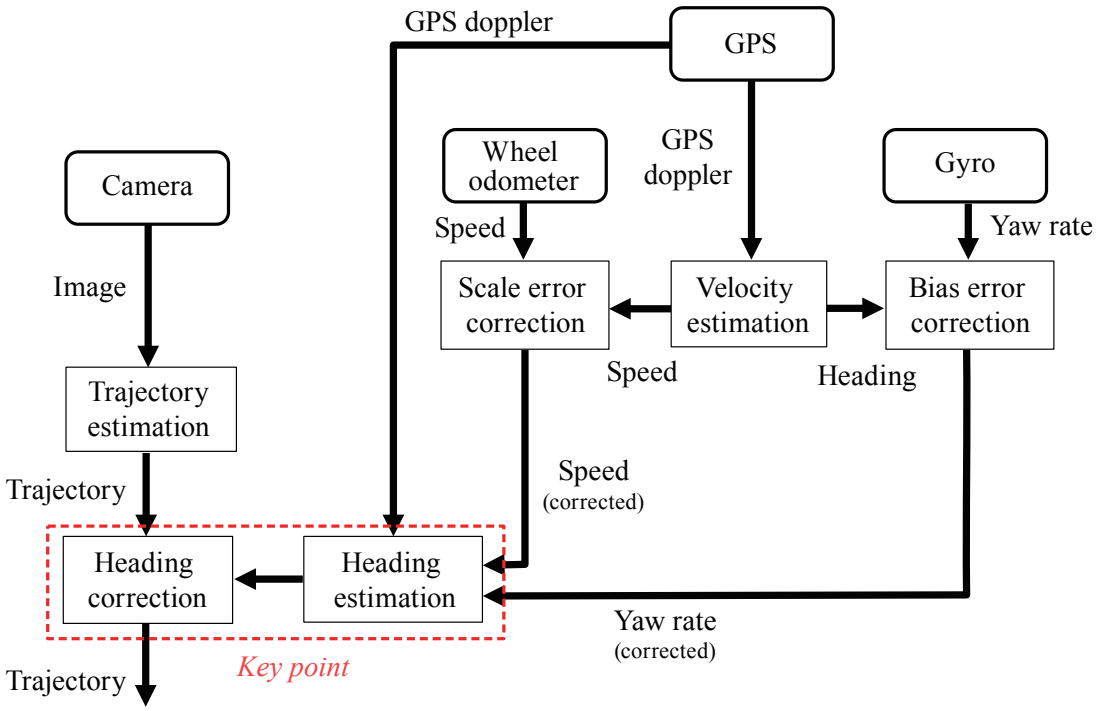

Fig. 4 Overview of the proposed method.

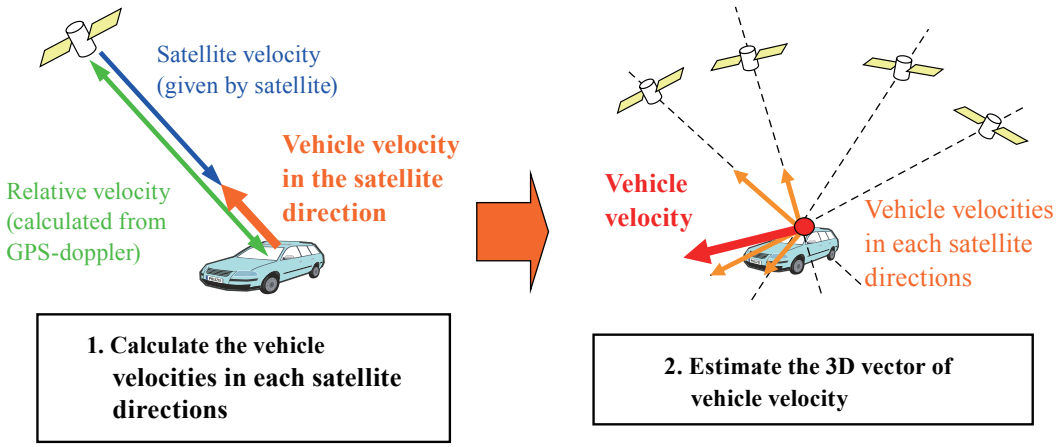

Fig. 5 Estimation of vehicle velocity using GPS Doppler.

the number of satellites observed in the current epoch. Thus, the equations can be solved when the number of satellites is four or more.

In the present study, the velocity vector estimated using GPS Doppler is used for sensor error correction of the IMU (**Fig. 6**). The size of the velocity vector (= vehicle speed) is used for scale error correction of the wheel speed, and the direction of the velocity vector (= vehicle heading) is used for bias error correction of the yaw rate of the gyro. These approaches to sensor error correction of the IMU are described below.

3. 3 Estimation of the Scale Error of Wheel Speed

Generally, the vehicle speed calculated from the wheel odometer (wheel speed) may have scale errors because the tire diameter changes over a long period owing to the change of pressure. The scale error of the wheel speed associated with the wheel speed accumulates with the distance traveled, and finally causes a large error in the distance traveled. In order to decrease the error accumulation in calculating the distance traveled, a technique that corrects the wheel speed error using the vehicle speed calculated from GPS Doppler (Doppler speed) is proposed.

Figure 7 shows an outline of the scale error correction of the wheel speed. The wheel speed is robust, but may have a scale error. On the other hand, the Doppler speed has some variation, but does not have a scale error. Thus, in the proposed method, noisy observations of Doppler speed are removed based on their variation during a recent short period, and the scale error of the wheel speed is then estimated by fitting the wheel speed to the Doppler speed using the least-squares method. The input time series data for the scale factor estimation is stored and updated when new data is obtained, and the scale value is also updated at that time. In this manner, the scale error of the wheel speed is repeatedly corrected.

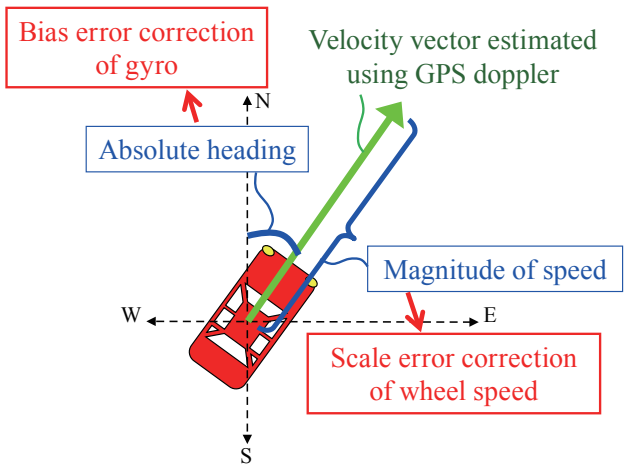

Fig. 6 Velocity vector for sensor error correction.

3. 4 Estimation of Bias Error of a Gyro

The yaw rate given by a gyro has a bias error. When calculating the vehicle heading by integrating yaw rates (yaw-rate heading), the bias error of yaw rate accumulates in the estimated vehicle heading. In order to decrease the accumulated heading error, a correction technique for the bias error of yaw rate using the vehicle heading calculated from GPS Doppler (Doppler heading) is proposed.

Figure 8 shows an outline of bias error correction of the gyro yaw rate. The yaw-rate heading is continuous, but has an accumulated error caused by a bias error in yaw-rate measurements. On the other hand, the Doppler heading has some variation but does not have a bias error. Thus, in the proposed method, the noisy observations of Doppler heading are removed based on their time variation during a recent short period, and the bias error of yaw rate is then estimated by fitting the yaw-rate heading to the Doppler heading using the least-squares method. As with speed scale estimation, the stored input data and the estimated bias value are both updated whenever new data are obtained, and the bias error is then corrected.

3. 5 Heading Estimation Using Time-series Tightly Coupled Integration of GPS Doppler and INS

In the previous sections, methods of IMU sensor calibration are described. In this section, a method of absolute heading estimation via integration of the GPS Doppler and the calibrated IMU is described. **Figure 9** shows the concept of absolute heading estimation using the proposed method. Time-series data of satellites are used to make up for the shortage of current satellite data. However, when using the time-series data, there is a problem that the number of unknown parameters describing the vehicle state at each epoch increases in proportion to the length of the time-series data, and this increases the uncertainty in the estimation. In order to avoid an increase in the number of unknown parameters with time, IMU is

used to place constraints on the time-series vehicle states. As a result, the proposed method can perform absolute heading estimation if only one satellite is observable at each epoch.

Next, the process of the proposed method is shown through equations. First, time-series observation values of GPS Doppler for M epochs are described as follows:

$$\frac{D_{t,i}}{f1}c + \mathbf{G}_{t,i} \cdot \mathbf{vs}_{t,i} = \mathbf{G}_{t,i} \cdot \mathbf{v}_t - c\rho_t \quad (t = 0, ..., M; \quad i = 1, ..., N_t), \tag{4}$$

where t (0, ..., M) is the time index of the time-series data, and N_t is the number of satellites at time t. Then, $\mathbf{v}_t$ is broken down into velocity magnitude and velocity direction as follows:

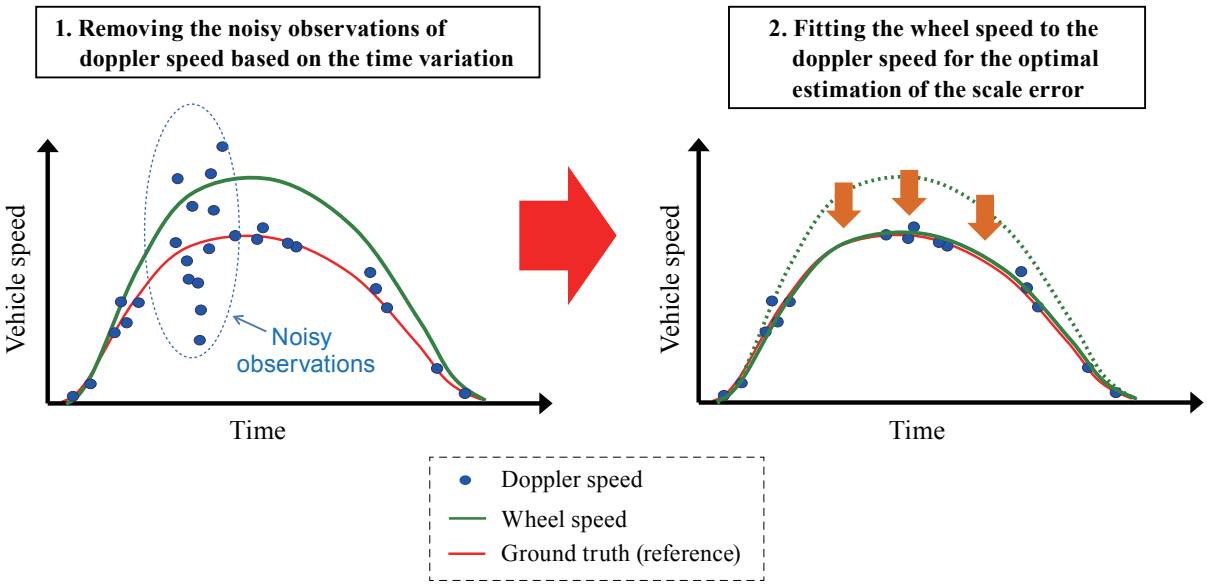

Fig. 7 Outline of the scale error correction of the wheel speed.

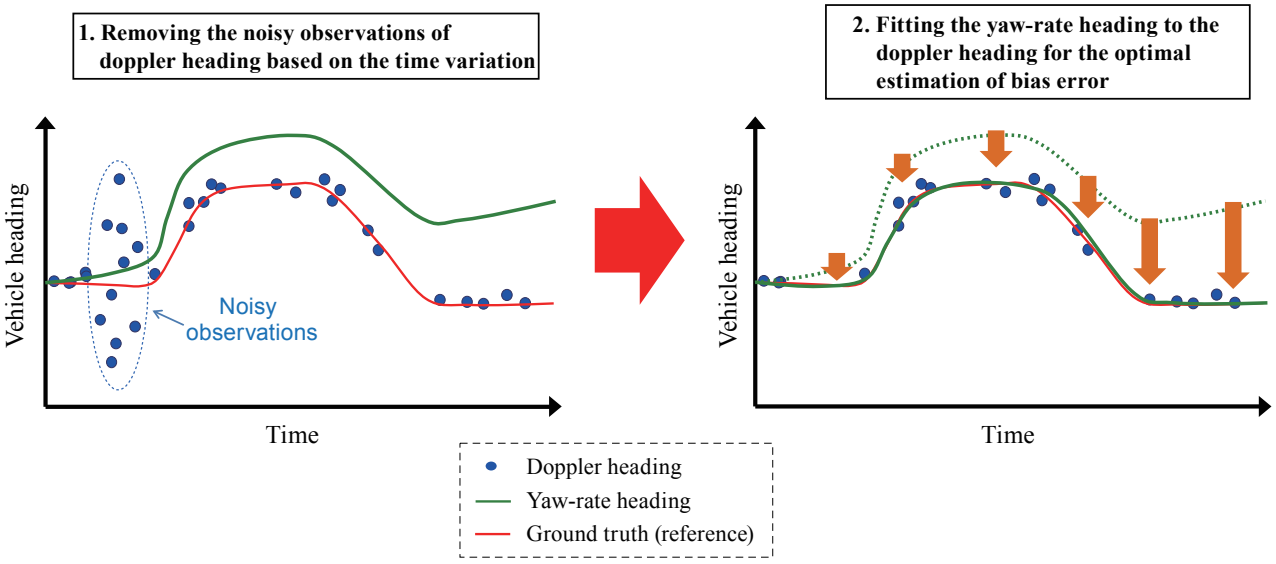

Fig. 8 Outline of the bias error correction of the gyro yaw rate.

$$\mathbf{v}_t = [Vx_t,\ Vy_t,\ Vz_t]$$
$$= |\mathbf{v}_t|\ [\cos\theta_t \cos\phi_t \quad \sin\theta_t \cos\phi_t \quad \sin\phi_t]\ , \qquad (5)$$

where $[Vx_t, Vy_t, Vz_t]$ are the components of the vehicle velocity vector in a planar coordinate system, $|\mathbf{v}_t|$ is the magnitude of velocity vector $\mathbf{v}_t$, θ_t is the heading angle of the vehicle, and ϕ_t is the elevation angle of the vehicle. The conditions of the constraint described below are then set in order to reduce the number of unknown parameters.

(a) The vehicle speed is constrained by the speed calculated from the wheel pulse rate.
(b) The time change of the vehicle heading angle is constrained by the yaw rate of the gyro.
(c) The vehicle elevation angle is always estimated to be 0. (The vehicle speed in the vertical direction is assumed to be negligibly small as compared to the vehicle speed in the horizontal direction).
(d) The time change of the clock drift is approximated to be linear because the time change of the clock error is generally very gradual.

These constraint conditions are as follows:

$$|\mathbf{v}_t| = Vw_t\ , \qquad (6)$$

$$\theta_t = \theta_0 - \Delta t \sum_{t'=0}^{t} \omega_{t'}\ , \qquad (7)$$

$$\phi_t = 0\ , \qquad (8)$$

$$\rho_t = \rho_0 - \alpha \cdot t\ , \qquad (9)$$

where Vw_t is the speed calculated from the wheel pulse rate, Δ_t is the processing time step, θ_0 is the vehicle heading at the current epoch, $\omega_{t'}$ is the yaw rate of the vehicle measured by gyro at time index t', ρ_0 is clock drift at the current epoch, α is the slope of the time change of the clock drift, and the unknowns are θ_0, ρ_0 and α. Then, by substituting Eqs. (5)-(9) into Eq. (4), we obtain the following:

$$\frac{D_{t,i}}{f1}c + \mathbf{G}_{t,i} \cdot \mathbf{vs}_{t,i} = Vw_t\, Gx_{t,i} \cos\left(\theta_0 - \Delta t \sum_{t'=0}^{t} \omega_{t'}\right) + Vw_t\, Gy_{t,i} \sin\left(\theta_0 - \Delta t \sum_{t'=0}^{t} \omega_{t'}\right) - c\,(\rho_0 - \alpha \cdot t)\ . \qquad (10)$$

In Eq. (10), the total number of unknowns is three (θ_0, ρ_0, α), and the total number of equations is equal to the total number of satellites in all time-series epochs. Thus, Eq. (10) can be solved, and the current heading of the vehicle θ_0 can be obtained if the total number of satellites during the entire time-series is three or more.

3. 6 Integration with VO

In this process, the absolute heading estimated by the proposed method is used to correct the heading of the VO, and then the trajectory of the VO is refined by the corrected headings.

First, the offset between the time-series heading of the VO and the absolute heading is calculated. Equation (11) shows the equation used to calculate the offset, where $\Delta\theta$ is the value of the offset, θ_t is the heading estimated by VO, φ_t is the absolute heading

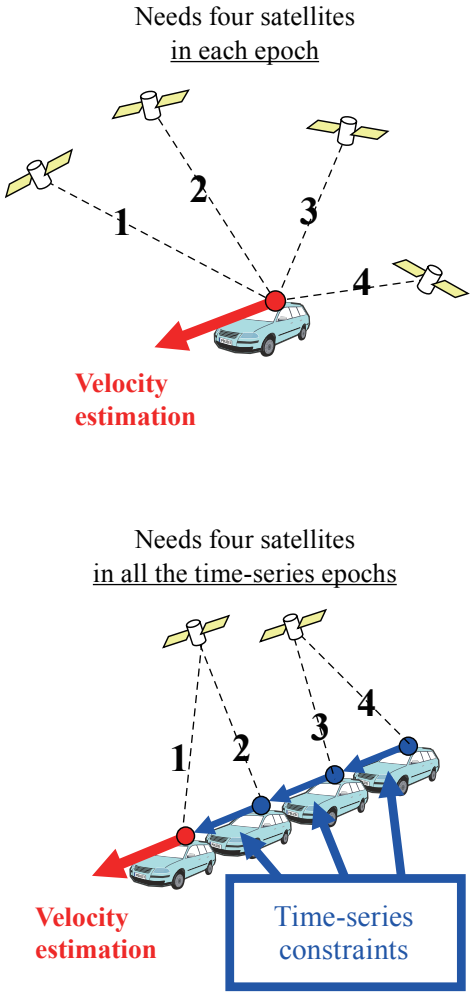

Fig. 9 Concept of absolute heading estimation using the proposed method.

estimated by the proposed method, δ_t is a flag that is 1 when the absolute heading can be obtained and is 0 otherwise, and t (0, ..., M) is the time index of the time-series data. The time-series headings estimated by VO are then corrected by adding the offset, as shown in Eq. (12). After the heading correction, the trajectory of VO is corrected as in Eq. (13). Here, $\mathbf{x}_t$ and $\tilde{\mathbf{x}}_t$ are the vehicle positions before and after the correction respectively, and $\mathbf{R}_t$ and $\tilde{\mathbf{R}}_t$ are the rotation matrices before and after the heading correction, respectively. The rotation matrix is a function of the rotation angles [pitch, yaw, roll]. Note that pitch and roll are not corrected in this process. Index $t = 0$ indicates the oldest time in the time-series data used for the estimation.

$$\Delta\theta = \sum_{t=0}^{M} \delta_t (\theta_t - \varphi_t) \Big/ \sum_{t=0}^{M} \delta_t \tag{11}$$

$$\tilde{\theta}_t = \theta_t + \Delta\theta \tag{12}$$

$$\tilde{\mathbf{x}}_t = \tilde{\mathbf{R}}_0 \, \mathbf{R}_0^{-1} \, (\mathbf{x}_t - \mathbf{x}_0) + \mathbf{x}_0 \tag{13}$$

4. Experiment

4. 1 Setup

Experiments were carried out in an urban area. **Table 1** shows the sensors used in the experiment. A gyro and a wheel odometer are included as standard equipment in the commercial vehicle used in the experiment, and their signals were captured through CAN BUS. Trimble NetR9 was used as the GPS receiver, and XCD-SX90 was used as the mono-camera. The resolution of the camera image is SXGA (1280 × 960). The angle of view of the camera is approximately 50 deg, and the camera direction is the same as the vehicle direction. As a reference positioning system, POSLV610[14] was used. The camera can measure the vehicle position with an accuracy of approximately 0.1 deg in urban environments. The output interval of each sensor is different, but the system ran with a minimum interval (without reference) of 12 ms. The data of the GPS and camera were synchronized to the closest epoch each time in 12 ms intervals. The amount of time-series data used for bundle adjustment was 30 epochs (= 2 s).

Table 1 Sensors used in the experiment.

Sensors	Product	Output interval
Gyro	Market vehicle	12 ms
Wheel odometer	Market vehicle	12 ms
GPS receiver	NetR9	50 ms
Camera	XCD-SX90 (SXGA)	66.7 ms
Reference system	POSLV610	5 ms

Figure 10 shows the evaluation course in Shinjuku City. The length of the evaluation course was approximately 500 m, and there were many high-rise buildings along the course.

4. 2 Results

Figure 11 shows the number of satellites and the error of heading estimation using the conventional method (GPS only) and the proposed method (tightly coupled integration of GPS/IMU). Heading estimation can be performed using the proposed method even when the number of satellites is less than four, whereas heading estimation cannot be performed in such situations using the conventional method. Moreover, the variance of the heading error is much lower with the proposed method owing to the increase in satellite information, which produces an averaging effect and enables the RAIM[15] method. In the present study, a reliability test for the estimated heading was performed based on the variance of the heading. The variance of the heading is calculated using subtraction between the gyro-based heading and the estimated heading for the past 10 epochs. As a result of the reliability test, some reliable headings are obtained using the proposed method, whereas reliable headings are not obtained using the conventional method.

Figure 12 shows the errors of heading and trajectory. VO + GPS is the VO integrated with the conventional method of heading estimation (GPS only), VO + GPS (TC) is the VO with the proposed method of heading estimation (tight coupling of GPS/IMU), and IMU + GPS (TC) is IMU-based trajectory estimation integrated with the proposed method of heading estimation. The heading error of VO + GPS increases as the vehicle progresses, which induces an increase in trajectory error. On the other hand, the heading error of VO + GPS (TC) is corrected in the latter half of the course, and the increase in trajectory error is suppressed.

Figure 13 shows the trajectory error per 100 m of

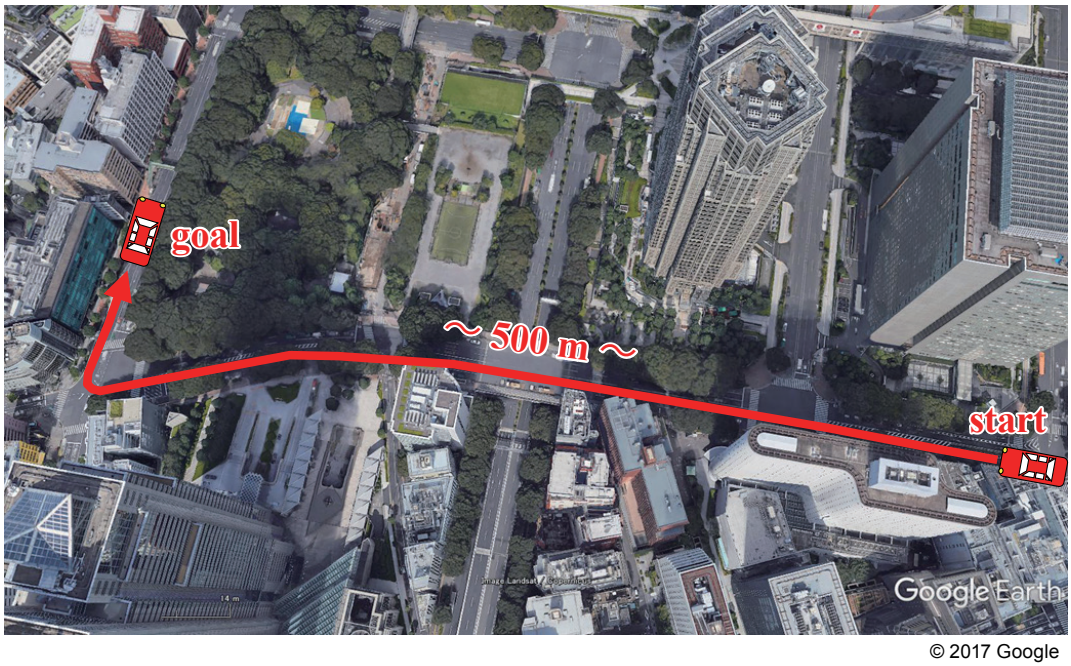

Fig. 10 Evaluation course in Shinjuku.

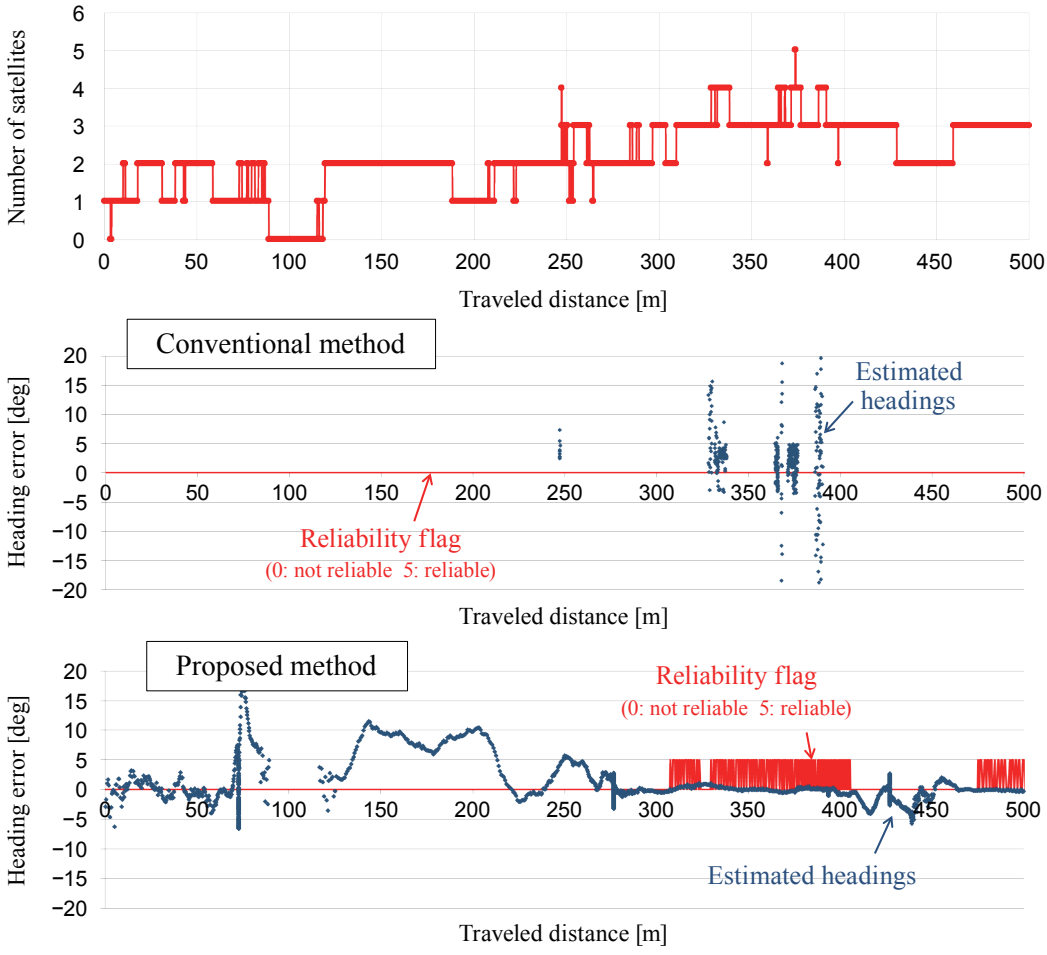

Fig. 11 Number of satellites and availability of absolute heading estimation.

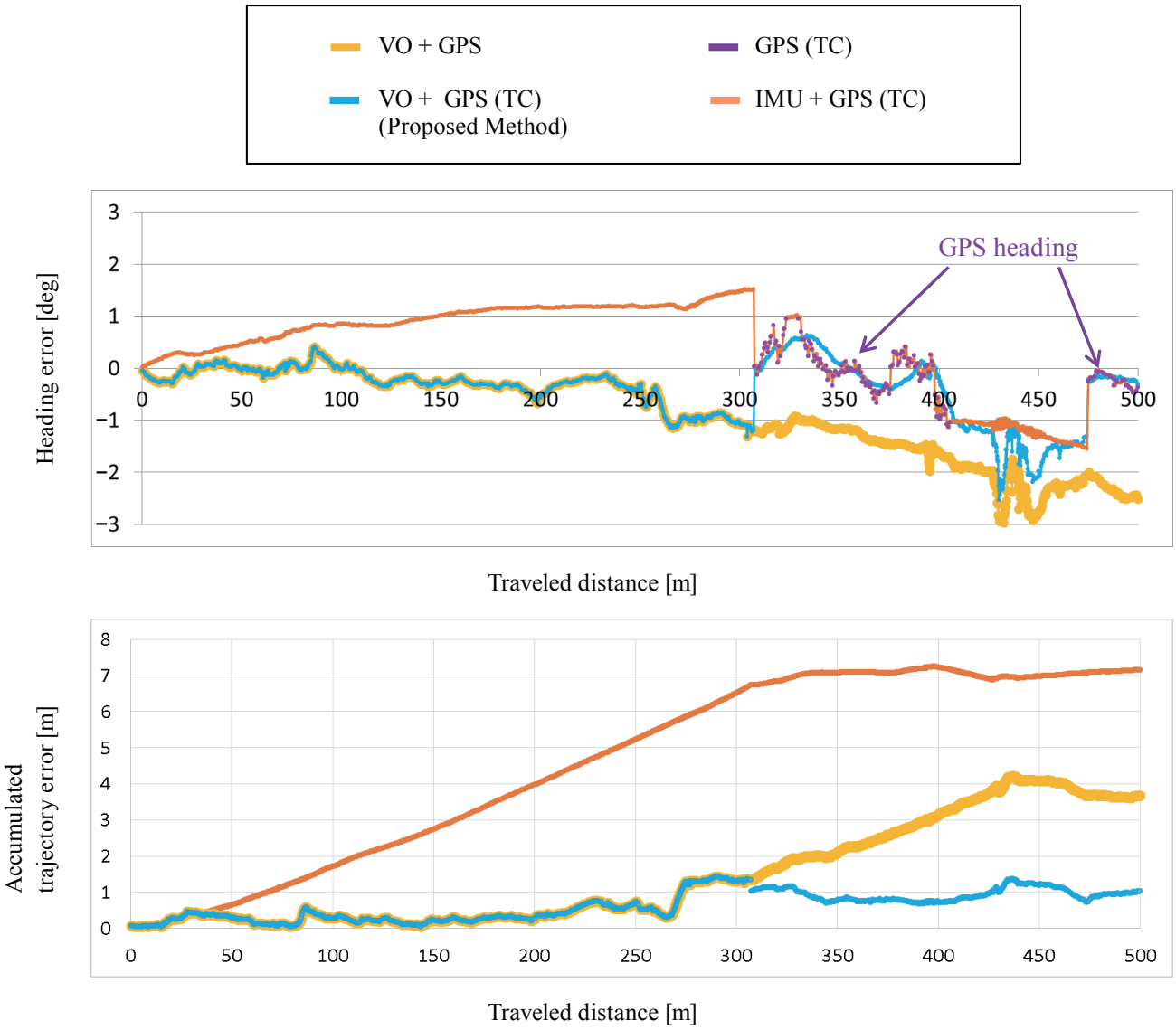

Fig. 12 Error of heading and trajectory.

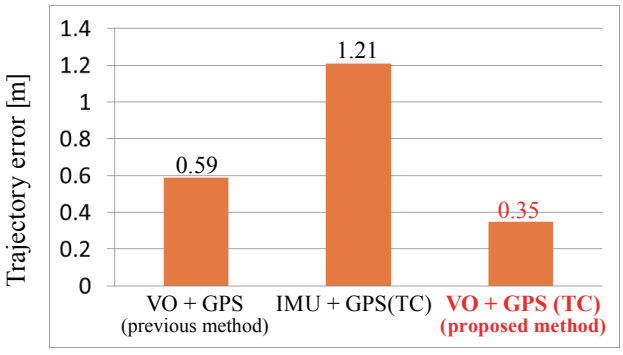

Fig. 13 Trajectory error per 100 m of driving.

driving. The trajectory error of the proposed method was approximately 40% less than that of the previous method (VO + GPS).

5. Conclusion

In the present study, a method that improves the accuracy of VO in urban environments by low-cost multi-sensor integration was proposed in which the key technique was heading estimation using the time-series tightly coupled integration of GPS/IMU. The proposed method contributes to the improvement of the heading estimation for cases in which the satellite reception is poor. Experiments in urban areas revealed that the trajectory error of the proposed method is reduced to approximately 1/4 of that of the conventional approach.

Reference

(1) Dai, L., Han, S., Wang, J. and Rizos, C., "A Study on GPS/GLONASS Multiple Reference Station Techniques for Precise Real-time Carrier Phase-based Positioning", *Proc. 14th Int. Tech. Meet. Satell. Div. Inst. Navigation* (2001), pp. 392-403.

(2) Burgard, W., Stachniss, C. and Hähnel, D., "Mobile Robot Map Learning from Range Data in Dynamic Environments", *Auton. Navigation in Dynamic Environ.* (2007), pp. 3-28, Springer.

(3) Alismail, H. S., Baker, L. D. and Browning, B., "Continuous Trajectory Estimation for 3D SLAM from Actuated Lidar", *Proc. IEEE Int. Conf. Rob. Autom.* (2014), pp. 6096-6101.

(4) Nister, D., Naroditsky, O. and Bergen, J., "Visual Odometry", *Proc. IEEE Comput. Soc. Conf. Comput. Vision and Pattern Recognit.*, Vol. 1 (2004), pp. I-652-I-659.

(5) Yamaguchi, K., Kato, T. and Ninomiya, Y., "Vehicle Ego-motion Estimation and Moving Object Detection Using a Monocular Camera", *Proc. 18th Int. Conf. Pattern Recognit.* (2006), pp. 610-613.

(6) Heng, L., Honegger, D., Lee, G. H., Meier, L., Tanskanen, P., Fraundorfer, F. and Pollefeys, M., "Autonomous Visual Mapping and Exploration with a Micro Aerial Vehicle", *J. Field Rob.*, Vol. 31, No. 4 (2014), pp. 654-675.

(7) Rehder, J., Gupta, K., Nuske, S. and Singh, S., "Global Pose Estimation with Limited GPS and Long Range Visual Odometry", *Proc. IEEE Int. Conf. Rob. Autom.* (2012), pp. 627-633.

(8) Meguro, J., Ishida, H., Guo, C. and Kojima, Y., "Road Ortho-image Generation and Road Marking Detection Using Conventional In-vehicle Sensors", *Proc. 20th ITS World Congr.*, No. 3010 (2013).

(9) Alonso, I. P., Llorca, D. F., Gavilán, M., Pardo, S. Á., García-Garrido, M. Á., Vlacic, L. and Sotelo, M. Á., "Accurate Global Localization Using Visual Odometry and Digital Maps on Urban Environments", *IEEE Trans. Intell. Transp. Syst.,* Vol. 13, No. 4 (2012), pp. 1535-1545.

(10) Triggs, B., McLuchlan, P. F., Hartley, R. I. and Fitzgibbon, A. W., "Bundle Adjustment: A Modern Synthesis", *Proc. IWVA 1999 Vision Algorithm: Theory and Practice* (2002), pp. 298-372.

(11) Marquardt, D. W., "An Algorithm for Least-squares Estimation of Nonlinear Parameters", *J. Soc. Ind. Appl. Math.*, Vol. 11, No. 2 (1963), pp. 431-441.

(12) Serrano, L., Kim, D., Langley, R. B., Itani, K. and Ueno, M., "A GPS Velocity Sensor: How Accurate Can It Be? –A First Look", *Proc. ION NTM* (2004), pp. 875-885.

(13) van Grass, F. and Soloviev, A., "Precise Velocity Estimation Using a Stand-alone GPS Receiver", *J. Inst. Navigation,* Vol. 51, No. 4 (2004), pp. 283-292.

(14) Applanix, "POSLV Specifications", <https://www.applanix.com/pdf/POSLV_Specifications_oct_2016_yw_(1).pdf>, (accessed 2017-10-06)

(15) Lee, Y. C., "Analysis of Range and Position Comparison Methods as a Means to Provide GPS Integrity in the User Receiver", *Proc. 42nd Annu. Meet. Inst. Navigation* (1986), pp. 1-4.

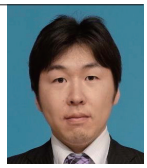

Kojiro Takeyama
Research Field:
- Navigation of Land Vehicles with Fusing Multi Sensors

Academic Societies:
- The Institute of Navigation
- The Institute of Electronics, Information and Communication Engineers
- Information Processing Society of Japan
- IEEE

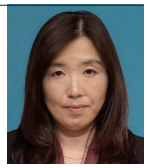

Yoshiko Kojima
Research Fields:
- Navigation of Land Vehicles Using Multiple Sensors
- Construction of Spatial Map for ADAS

Academic Degree: Ph.D.
Academic Societies:
- The Institute of Electronics, Information and Communication Engineers
- Information Processing Society of Japan
- IEEE

Awards:
- IPSJ Yamashita SIG Research Award, 2002
- IPSJ Best Paper Award, 2002
- Best Paper Award, 10th International Symposium on Advanced Vehicle Control, 2010

